Hindawi
Advances in Materials Science and Engineering
Volume 2019, Article ID 4562958, 8 pages
https://doi.org/10.1155/2019/4562958

Research Article

Thermal Conductivity of Dry Sands Treated with Microbial-Induced Calcium Carbonate Precipitation

Zhaoyu Wang,[1] Nan Zhang,[2] Fei Lin,[1] Jinhua Ding,[3] and Huimin Yang[1]

[1]*College of Civil Engineering, Yancheng Institute of Technology, Yancheng, Jiangsu 224051, China*
[2]*Department of Civil Engineering, The University of Texas at Arlington, Arlington, Texas 76019, USA*
[3]*College of Civil Engineering, Jiangsu University of Science and Technology, Zhenjiang, Jiangsu 212003, China*

Correspondence should be addressed to Nan Zhang; zhangnanvictor47@hotmail.com

Received 9 November 2018; Accepted 9 January 2019; Published 3 February 2019

Academic Editor: Necmettin Maraşlı

With an increasing energy demand, exploration and utilization of new energy resources become more significant recently. Geothermal energy, characterized as a clean, renewable, and sustainable energy, has various engineering applications. Microbial-induced calcium carbonate precipitation (MICP) technique has a potential to improve soil thermal properties for geothermal applications. In this study, thermal conductivity of dry sands treated using MICP technique with different treatment cycles was investigated in laboratory. The results showed that thermal conductivity of MICP-treated sands was much higher than that of the untreated sand under dry condition and it increased with increasing treatment cycles. Based on the scanning electron microscopy (SEM) analyses, it is found MICP-induced $CaCO_3$ crystals are being formed among sand particles functioned as "thermal bridge," which provided more highly effective heat transfer path. It is concluded that the MICP technique could significantly improve the thermal conductivity of sands and the overall heat transfer efficiency. It is advantageous to use MICP-treated soils as enhanced grout materials for underground energy geostructures.

1. Introduction

The current energy structure mainly relies on the coal; thereby, the exploration of new energy resources for energy conservation and reduction of CO_2 emission is urgent in the world. Geothermal energy is a clean, renewable, and sustainable energy resource, which has various engineering applications, such as ground source heat pumps (GSHPs) and geothermal energy piles (GEPs) [1]. The performance of such underground energy structures is strongly affected by the saturation degree of soils [2]. It is found that low saturation degree reduced soil thermal conductivity, which lowered the efficiency of heat exchange between soils and the structures [3]. Geothermal energy has also been used in temperate or subtropical areas like Turkey [4], but it is still undeveloped in arid areas because of the relatively low saturation degree of soils. Hence, it is necessary to explore an innovative way to improve soil thermal conductivity under nearly dry condition in arid areas in order to expand geothermal applications.

Microbial-induced calcium carbonate precipitation (MICP) technique aims to produce $CaCO_3$ precipitation in the environment containing a large amount of Ca^{2+} through hydrolysis of urea by bacteria for in situ cementation of soils [5, 6]. It is indicated that the porosity of MICP-treated soils will be reduced, resulting in a decrease of soil permeability. As a result, the flow of water in pore space of soils will be affected [7]. It is also found that the permeability was decreased by an order of magnitude after one cycle of MICP treatment [8]. Additionally, the unconfined compressive strength of MICP-treated sands was significantly improved [9]. Van Paassen et al. [10] proved the feasibility of using MICP technique to reinforce soils based on a series of large-scale laboratory tests. The main advantage of the technique is that it can replace the cementitious materials for reinforcing soils without causing potential detrimental impact on natural environment.

Soil thermal properties include thermal conductivity, thermal diffusivity, and specific heat capacity. Temperature distribution and efficiency of heat conduction in soils are mainly affected by its thermal conductivity [11]. Soil thermal conductivity is also the most important soil property for the design of underground energy structures for geothermal applications. Choi et al. [12] stated that the heat exchange efficiency of saturated soils was increased by 40% as compared with that of dry soils. Venuleo et al. [2] found that thermal conductivity of MICP-treated soils was increased by 250% as compared with untreated soils. It is most probably attributed to the fact that MICP-induced $CaCO_3$ crystals in soils increased the contact area and the number of heat transfer path among soil particles. However, the study on thermal conductivity of sand treated by the MICP technique under dry condition is still rare and the micromechanism of heat conduction in MICP-treated sands is not well understood.

In this study, thermal conductivity of MICP-treated sands under dry condition was first measured by a single thermal probe using the transient-state method. The effect of MICP treatment cycles on thermal conductivity of dry sands was also investigated. Additionally, the micromechanism of heat conduction in MICP-treated sands was presented based on the scanning electron microscopy (SEM) analyses.

2. Materials and Methods

2.1. Test Sand. Test sand was taken from a construction site and then sieved to remove any cobbles in laboratory. The sand is characterized as poorly graded fine sand (SP) according to the unified soil classification system (USCS). The properties of sand are shown in Table 1. The gradation curve is shown in Figure 1. The test sand was washed and then oven-dried at 105°C for 8 hours to avoid any interference from antecedent microbial or plant communities for future experiments.

2.2. Preparation of Nutrient Solution. Nutrient solution contains nutrients needed for growth of microorganisms, and the amount of nutrients has a great impact on the quality of microorganisms. The procedures for preparing nutrient solution are as follows: (1) predetermined mass of each component (i.e., tryptone, soya peptone, NaCl, and urea, as shown in Table 2) was prepared and poured into a clean, dry conical bottle. Then, a certain amount of purified water was added into the bottle and mixed with each component thoroughly; (2) NaOH solution with a concentration of 5 mol/L was added in the bottle in the proportion of 200 ml NaOH solution to 100 ml nutrient solution to adjust the pH value of nutrient solution in the range 7.0–7.5 using a pH reading device; (3) the conical bottle was shook to ensure that each component was completely dissolved, and the nutrient solution was transparent without obvious precipitation and suspension; and (4) The prepared nutrient solution was transferred into a high-pressure steam sterilizer for sterilization for 20 min at 120°C. Then, the solution was allowed to cool down to room temperature in the sterilizer and taken out for future tests.

Table 1: Properties of test sand.

Name	D_{50} (mm)	G_s	C_c	C_u	e_{max}	e_{min}
Sand (SP)	0.35	2.65	1.04	2.67	0.88	0.62

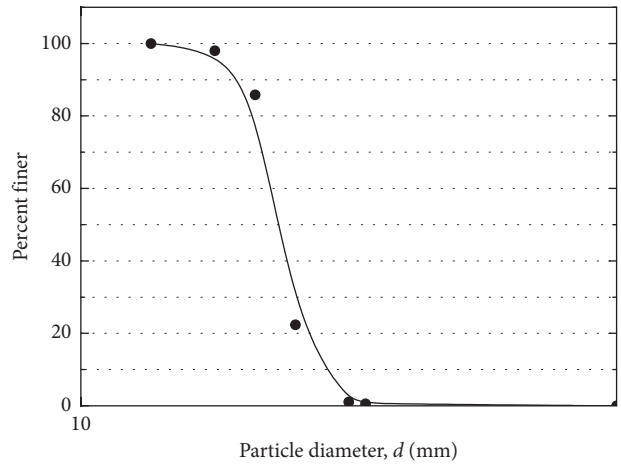

Figure 1: Gradation curve of test sand.

2.3. Preparation of Bacterial Solution. The bacterial solution was obtained by the culture of bacteria in the nutrient solution. *Sporosarcina pasteurii* was selected as the bacterial species in this study. It is necessary to do aseptic operation when preparing bacterial solution. The ultraviolet lamp was first opened for 2 hours in a sterile table and then closed for preparation of bacterial solution. Then, the prepared nutrient solution was placed in the table with the fluorescent lamp, and the fan was opened. The *Sporosarcina pasteurii* species in the cryopreservation tube was transferred into the nutrient solution using a pipette in the proportion of 1 ml liquid strain to 100 ml nutrient solution. The prepared bacterial solution was then placed in a shaking table at a temperature of 30°C and speed of 130 rpm for 30 hours for the culture of bacteria. The OD_{600} values of different batches of bacterial solutions were measured using a UV-2000 spectrophotometer before the MICP treatment, and they were found to be very close (i.e., around 1.7). It meant that the concentration of the bacterial solutions was identical, and the effect of concentration of solutions on the effectiveness of MICP treatment can be neglected.

2.4. Preparation of Cementation Solution. The cementation solution provides sufficient Ca^{2+} and enough urea for microorganisms to produce CO_3^{2-}, and Ca^{2+} reacts with CO_3^{2-} to produce $CaCO_3$ during MICP treatment. Previous test results showed that $CaCO_3$ can be effectively generated by using cementation solution with a concentration of 1.0 mol/L. In this study, dry urea and anhydrous calcium chloride were first mixed in proportions and then dissolved in a certain amount of purified water to prepare cementation solution with the same concentration. Content of each component in cementation solution is presented in Table 3.

Table 2: Content of each component in nutrient solution.

Name	Purified water (ml)	Tryptone (g)	Soya peptone (g)	NaCl (g)	Urea (g)
Content	100	1.5	0.5	0.5	6

Table 3: Content of each component in cementation solution.

Name	Purified water (ml)	Urea (g)	Anhydrous $CaCl_2$ (g)
Content	100	6	11.1

2.5. Preparation of MICP-Treated Sands. Preparation of MICP-treated sands was performed in a plastic syringe with an inner diameter of 38 mm and a height of 100 mm. The schematic of experimental setup is shown in Figure 2. It consisted of a collection pool, a plastic syringe, a peristaltic pump, and a conical bottle. Rubber stopples, gauzes, and porous stones were also used for sample preparation. As shown in Figure 2, the bacterial/cementation solution was injected into the sand sample from the bottom to top by the peristaltic pump, and the effluent solution was collected in the collection pool.

The procedures of sample preparation are as follows: (1) A 4 mm thick porous stone was first placed at the bottom of the syringe, and a 5 mm thick gauze was placed above it to prevent sand from flowing into the grouting tube; (2) test sand was poured into the syringe in four equal layers and slightly compacted to a total height of 80 mm. The initial dry density of dry sand sample was 1.50 g/cm^3; (3) another 5 mm thick gauze was placed on top of the sand sample. A rubber stopple was plugged into the syringe from the top to be in contact with the gauze to make sure the syringe was sealed. Then, the syringe was fixed vertically on a test frame; (4) 100 mL of purified water was continuously injected into the sand sample at a rate of 5 mL/min using the pump to remove the trapped air among sand particles; (5) 100 mL of bacterial solution was then injected into the sand sample at the same rate. The valve was closed for 2 hours to allow bacteria to be uniformly distributed and adhered on sand particles; (6) the valve was opened to remove the residual solution in the tube. 100 mL of cementation solution was then injected into the sand sample at the same rate. The valve was again closed for 6 hours to ensure the biochemical reaction was completed; (7) the valve was again opened to remove the residual solution. This entire process represents one MICP treatment cycle. The sand sample was then cured at room temperature (i.e., 30 ± 2°C) for 20 days; (8) the porous stone, gauze, and rubber stopple were removed, and the MICP-treated sand sample along with the syringe was transferred into an oven at a temperature of 108°C for 8 hours. The dry MICP-treated sand sample was ready for the thermal conductivity measurements; (9) procedures (5), (6), (7), and (8) were repeated to prepare MICP-treated sand samples with other treatment cycles (i.e., 2, 3, and 4).

2.6. Measurement of Thermal Conductivity. The transient-state method had been widely used to measure thermal properties of soils in literature [13, 14], and it was adopted to measure thermal conductivity of MICP-treated sands under dry condition in this study by using a single thermal probe as shown in Figure 3. The probe consisted of a stainless-steel tube, a resistance wire, two electrical wires, a thermocouple, and thermoepoxy. The design criteria and fabrication process referred to Yu et al.'s study [15].

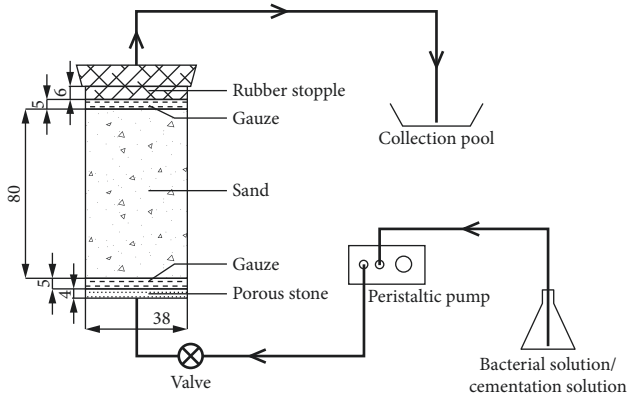

Figure 2: Schematic of experimental setup for preparation of MICP-treated sand (unit: mm).

Figure 4 shows the schematic of experiment setup for thermal conductivity measurement. The thermal probe was connected to a DC current source, i.e., IVYTECH 3605. It was used to generate a short heat pulse to heat the sand sample. The thermocouple was connected to a temperature readout unit, i.e., TC-08, to monitor temperature variations. The recorded temperature variations were eventually used to determine sand thermal conductivity.

Test procedures of thermal conductivity measurement are described below: (1) due to the relatively high stiffness of the MICP-treated sands, a hole with a diameter of 0.18 mm was predrilled vertically at the center of the top surface of the sand sample; (2) the thermal grease was spread on the surface of the thermal probe, and then, the probe was vertically inserted into the hole for measurements of sand thermal conductivity; (3) a current of 0.1 amp was applied for 300 s to heat the sand sample, and the temperature variation was recorded in the heating and cooling processes. It is noted that thermal conductivity of the untreated dry sand sample with the same initial dry density (i.e., 1.50 g/cm^3) was also measured for comparison.

According to the line heat source theory, the temperature rise of the probe (ΔT) depends on the heating power (Q) and the soil thermal conductivity (k). The thermal conductivity can be calculated by the following equation:

$$k = \frac{(q)/(4\pi)}{(dT)/(d(\ln t))}, \quad (1)$$

where $q = I^2R/L$; I is the applied current (amp); R is the resistance of the resistance wire (Ω); L is the length of the

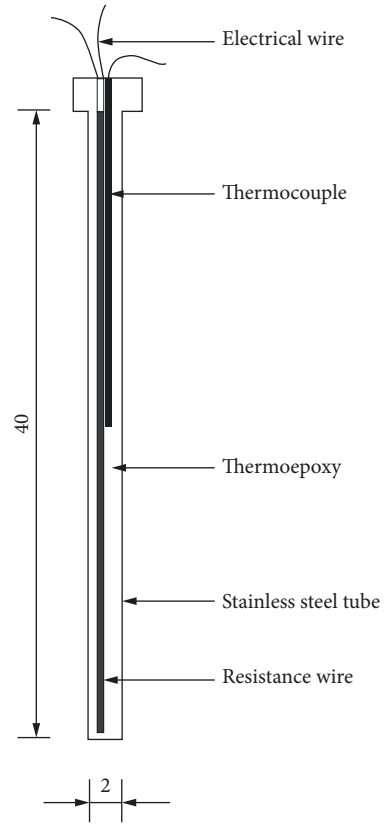

Figure 3: Schematic of the single thermal probe (unit: mm).

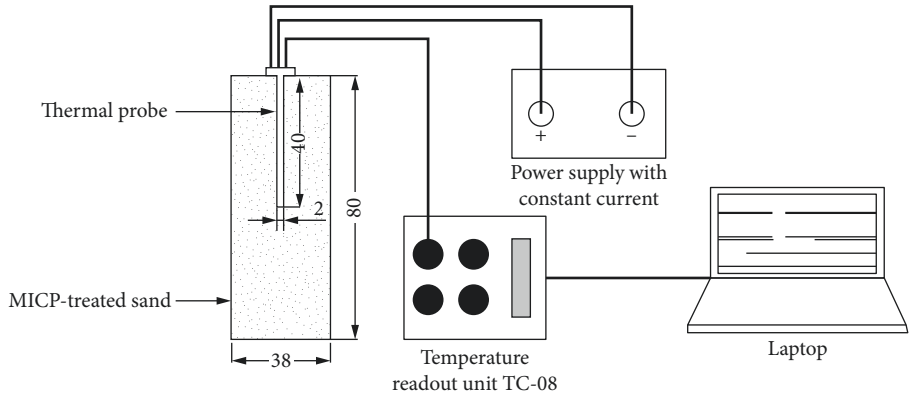

Figure 4: Schematic of experiment setup for thermal conductivity measurement (unit: mm).

probe (m); T is the recorded temperature (°C); and t is the heating time (s).

Figure 5 shows the variation of temperature with heating time of the single thermal probe [16]. It is indicated that the temperature variation can be divided into three stages: (1) the heating process of the probe itself (i.e., transient state); (2) the heat conduction from the probe to the surrounding pore fluid (i.e., transient to steady state); (3) the heat conduction after a steady temperature gradient is achieved in the surrounding medium. In the three stages, the thermal conductivity increases step by step, so the rate of temperature rise decreases gradually. Temperature (T) is linearly correlated with lnt only in the second stage [17]. Based on the recorded temperature variation and time, the data were fitted by the linear equation $T = a\ln t + b$ in the software Origin 8.0, so $dT/d(\ln t)$ in equation (1) equals to a. Then, soil thermal conductivity can be calculated accordingly. Using this method, the thermal probe was first calibrated in glycerol ($C_3H_8O_3$) of 99 % purity. It is found that the maximum absolute error between actual thermal conductivity of glycerol (i.e., 0.358 $W \cdot m^{-1} \cdot K^{-1}$) and the measured values was only within 0.005 $W \cdot m^{-1} \cdot K^{-1}$ from multiple tests.

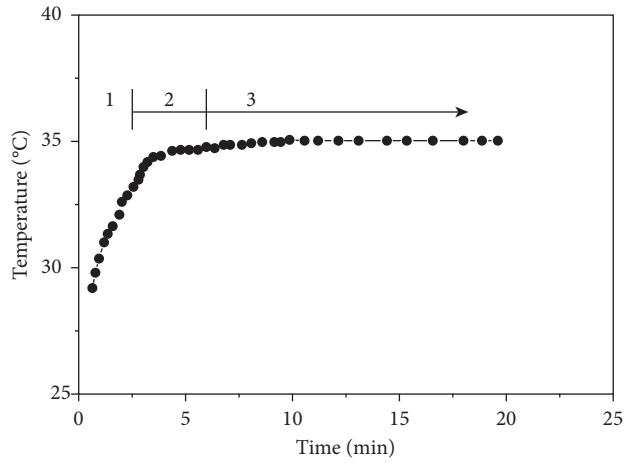

Figure 5: Variation of temperature with heating time of the single thermal probe [16].

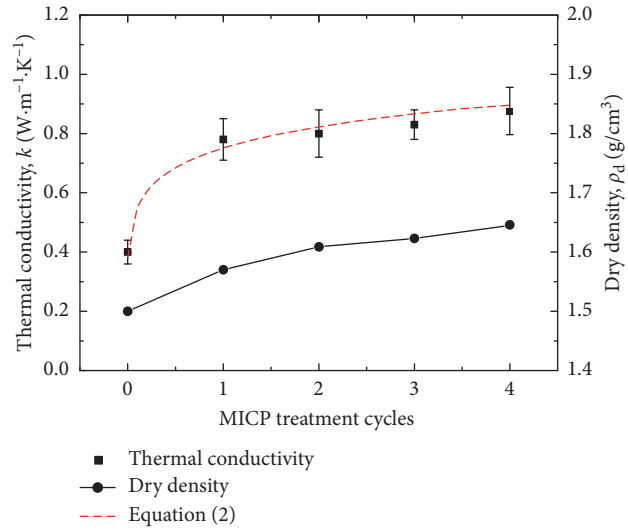

Figure 6: Measured thermal conductivity, dry density of MICP-treated sand, and MICP treatment cycles.

3. Results and Discussion

Thermal conductivity and dry density of MICP-treated sand under dry condition with different treatment cycles are depicted in Figure 6. It is indicated that thermal conductivity of MICP-treated sands was much higher than that of the untreated sand, and it slightly increased with the treatment cycles. Additionally, thermal conductivity of the MICP-treated sands with one to four treatment cycles was increased by 95%, 100%, 107.5%, and 120% as compared to the untreated sand, respectively. The measured data were fitted by an exponential function as shown in equation (2) to express the relationship between thermal conductivity of sand under dry condition and the MICP treatment cycles:

$$k_{\text{dry}} = e^{(0.1\times\ln(N+0.01))} - 0.25. \quad (2)$$

In addition, dry density of MICP-treated sands also increased gradually with the treatment cycles as shown in Figure 6. It is mainly because the dry weight of the sand sample was increased due to the generated $CaCO_3$ precipitation after the MICP treatment. With the total volume of the sample remaining unchanged, the dry density of MICP-treated sand was increased. Moreover, the maximum dry density was found to be 1.645 g/cm^3 for the treated sand with four treatment cycles. The dry density of the MICP-treated sand with one to four treatment cycles was increased by 4.7%, 7.2%, 8.2%, and 9.6% as compared to the untreated sand, respectively.

Figure 7 shows the relationship between thermal conductivity of MICP-treated sands and dry density. The predicted thermal conductivity of dry sand by the Johansen [18] model is also depicted in the figure. It is indicated that the measured thermal conductivity of MICP-treated sands slightly increased with the dry density. Thermal conductivity of untreated sand was found to be higher than the predicted value, which might be attributed to the measurement error.

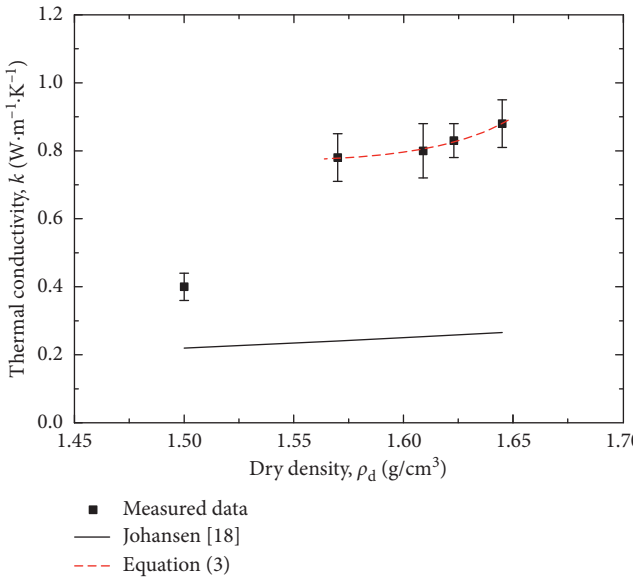

Figure 7: Measured thermal conductivity of MICP-treated sand and dry density.

However, the Johansen [18] model significantly underestimated thermal conductivity of treated sand in the dry density range $1.57 < \rho_d < 1.65$ g/cm^3, which also revealed that the unsuitability of existing thermal conductivity models for MICP-treated soils. An exponential function was used to fit the data to describe the relationship between thermal conductivity of MICP-treated sands and dry density under dry condition:

$$k_{\text{dry}} = 1.37\times10^{-22}\times e^{\rho_d/0.034} + 0.765. \quad (3)$$

Cote and Konrad [19] analyzed the relation between porosity and thermal conductivity of dry soils based on a large dataset of measured thermal conductivity in literature and proposed a new model to predict thermal conductivity of dry soils as follows:

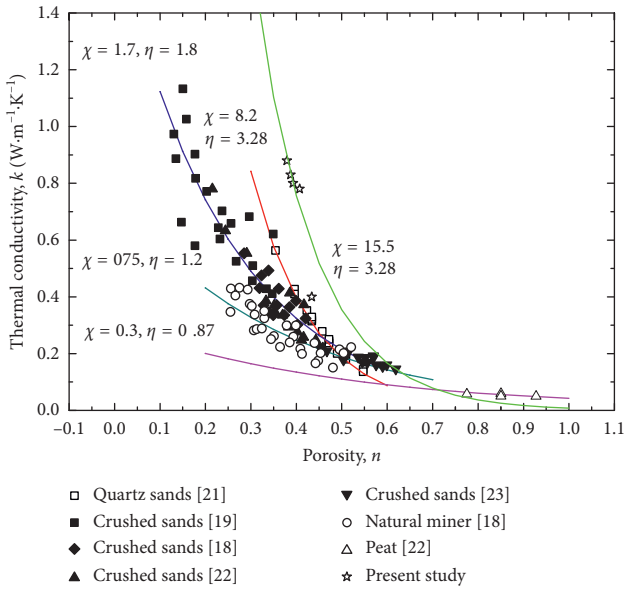

Figure 8: Measured soil thermal conductivity and porosity (comparison between natural soils and MICP-treated sand).

$$k_{\text{dry}} = \chi 10^{-\eta n}, \tag{4}$$

where χ and η are the coefficients accounting for the soil type and grain shape effects on thermal conductivity of dry soils and n is the porosity of soils.

As reported by Cote and Konrad [19], the values of χ and η are, respectively, 1.7 $W{\cdot}m^{-1}{\cdot}K^{-1}$ and 1.8 for crushed rocks, 0.75 $W{\cdot}m^{-1}{\cdot}K^{-1}$ and 1.2 for natural mineral soils, and 0.3 $m^{-1}{\cdot}K^{-1}$ and 0.87 for organic fibrous soil (peat) (Figure 8). Thereafter, Zhang et al. [20] proposed two new suggested values (i.e., 8.12 $W{\cdot}m^{-1}{\cdot}K^{-1}$ and 3.28) for quartz sands based on a series of laboratory experiments (Figure 8). In this study, the best fitting curve for MICP-treated sands was obtained with χ and η values of 15.5 $W{\cdot}m^{-1}{\cdot}K^{-1}$ and 3.28 as shown in Figure 8. These two values are higher than the suggested values proposed by Cote and Konrad [19] and Zhang et al. [20] for quartz sands and fine and medium sands and even much higher than others for silty soils, clayey soils, silts, and clays. It is noted that the measured thermal conductivity of untreated sand much deviated from the new fitted curve for MICP-treated sands, but it was very close to the one for quartz sands from Chen's study [21], which is because the test sand contains relatively high quartz content. In comparison, the quartz content of test sands was relatively lower than that reported in Kersten and Smith's studies [22, 23].

Scanning electron microscopy (SEM) technique was adopted to further study the micromechanism of heat conduction in MICP-treated sands. Figure 9(a) shows the image of untreated sand at magnification of 300x, and Figures 9(b)–9(d) show the images of MICP-treated sands with two treatment cycles at magnifications of 500x, 1000x, 3000x, respectively. In Figure 9(a), it is observed that the sand particles were packed randomly with smooth surface, and they were mainly in "point-to-point" contact with relatively small contact area. In contrast, $CaCO_3$ was observed in pore space among sand particles in MICP-treated sands as shown in Figures 9(b)–9(d). As known, thermal conductivity of $CaCO_3$ is much greater than the air (around 0.026 $W{\cdot}m^{-1}{\cdot}K^{-1}$). Thus, for sand under dry condition, the produced $CaCO_3$ replaced the air and functioned as "thermal bridge" to provide more highly conductive heat transfer path by increasing the contact area among sand particles as shown in Figure 10. As a result, thermal conductivity of MICP-treated sands significantly increased. Another reason is that thermal conductivity of water (around 0.59 $W{\cdot}m^{-1}{\cdot}K^{-1}$) is much higher than the air, so heat conduction in sands under dry condition mainly occurs inside sand particles or between different sand particles. As presented previously, with the same dry density or porosity, thermal conductivity of MICP-treated sands is higher than that of the untreated sand, which is also due to the "thermal bridge" effect on heat conduction. Besides, as the number of MICP treatment cycles increases, the amount of produced $CaCO_3$ increases, which had been proved by the increase of dry density of sand samples as shown in Figure 6. Consequently, such "thermal bridge" effect will be more prominent on the improvement of sand thermal conductivity under dry condition.

4. Conclusions

In this study, thermal conductivity of MICP-treated sands under dry condition was investigated using a single thermal probe based on the transient state method. The effect of MICP treatment cycles on measured thermal conductivity was also discussed. It is concluded that thermal conductivity of MICP-treated sands was much higher than that of the untreated sand sample under dry condition, and it was increased by 95%, 100%, 107.5%, and 120% as compared to the untreated sand sample for the four different treatment cycles. The dry density of the MICP-treated sands with one to four treatment cycles was increased by 4.7%, 7.2%, 8.2%,

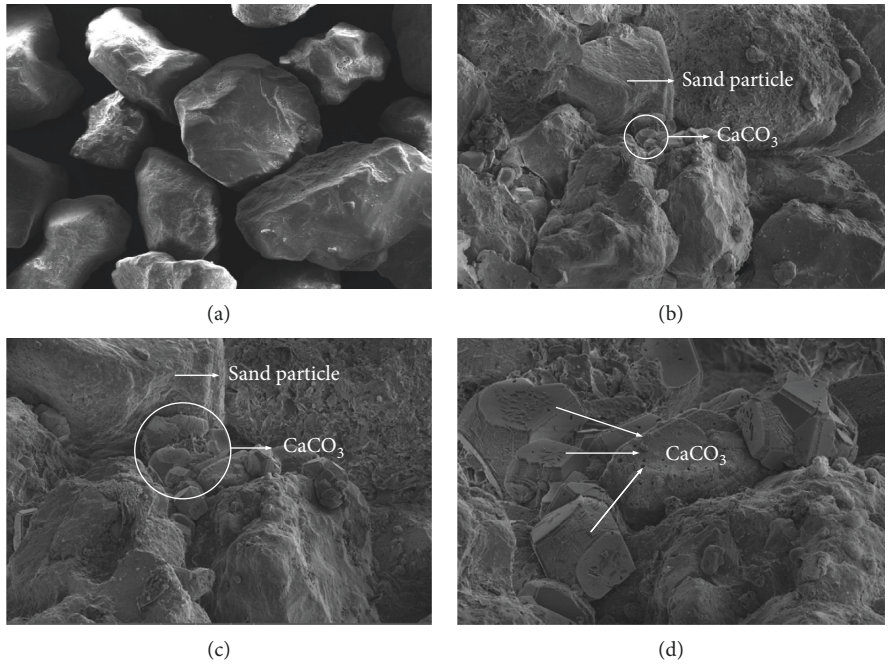

Figure 9: SEM images of pure sands and MICP-treated sand. (a) Untreated sand at magnification of 300x. (b) MICP-treated sand at magnification of 500x. (c) MICP-treated sand at magnification of 1000x. (d) MICP-treated sand at magnification of 3000x.

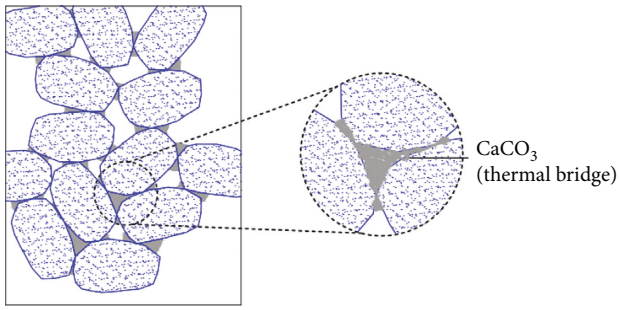

Figure 10: Schematic of "thermal bridge" in MICP-treated sand.

and 9.6% as compared to the untreated sand. Based on the SEM analyses, the "thermal bridge" effect caused by the produced $CaCO_3$ is the fundamental micromechanism for the improvement of sand thermal conductivity. The use of MICP technique to enhance heat transfer efficiency in sands at low saturation degree or nearly dry condition is feasible, and the MICP-treated soils has a great potential to be used as enhanced grout materials in GSHPs and GEPs for geothermal applications.

Data Availability

The data used to support the findings of this study are available from the corresponding author upon request.

Conflicts of Interest

The authors declare that there are no conflicts of interest regarding the publication of this paper.

Acknowledgments

This research was financially supported by the Natural Science Foundation of Jiangsu Province (Grant no. BK20161311), the Six Major Talent Peak in Jiangsu Province in China (Grant no. 2015-JZ-011), the Joint Technology Transfer Center of Yancheng Vocational Institute of Industry Technology, Yancheng Polytechnic College (Grant no. YGKF-201705), and the Innovation of Science and Technology of Institution of Higher Education in Jiangsu Province (Grant no. 2017-51).

References

[1] N. Zhang, X. Yu, A. Pradhan, and A. J. Puppala, "A new generalized soil thermal conductivity model for sand-kaolin clay mixtures using thermo-time domain reflectometry probe test," *Acta Geotechnica*, vol. 12, no. 4, pp. 739–752, 2017.

[2] S. Venuleo, L. Laloui, D. Terzis, T. Hueckel, and M. Hassan, "Microbially induced calcite precipitation on soil thermal conductivity," *Géotechnique Letters*, vol. 6, no. 1, pp. 39–44, 2015.

[3] J. K. Arthur and A. Kantzas, "Evaluating the effects of grain statistics, porosity and saturation on thermal conductivity of oil sands," in *Proceedings of AAPG Annual Convention and Exhibition*, Calgary, Alberta, Canada, June 2016.

[4] A. Hepbasli, O. Akdemir, and E. Hancioglu, "Experimental study of a closed loop vertical ground source heat pump system," *Energy Conversion and Management*, vol. 44, no. 4, pp. 527–548, 2003.

[5] B. M. Mortensen and J. T. DeJong, "Strength and stiffness of MICP treated sand subjected to various stress paths," in *Proceedings of Geo-Frontiers 2011*, pp. 4012–4020, Dallas, TX, USA, March 2011.

[6] Z. Y. Wang, N. Zhang, G. J. Cai, Y. Jin, N. Ding, and D. J. Shen, "Review of ground improvement using microbial induced carbonate precipitation (MICP)," *Marine Georesources & Geotechnology*, vol. 35, no. 8, pp. 1135–1146, 2017.

[7] W. K. V. Wijngaarden, F. J. Vermolen, G. A. M. V. Meurs, and C. Vuik, "Modelling biogrout: a new ground improvement method based on microbial-induced carbonate precipitation," *Transport in Porous Media*, vol. 87, no. 2, pp. 397–420, 2011.

[8] R. Shahrokhi-Shahraki, B. C. O'Kelly, A. Niazi, and S. M. A. Zomorodian, "Improving sand with microbial-induced carbonate precipitation," in *Proceedings of the Institution of Civil Engineers Ground Improvement*, vol. 168, no. 3, pp. 217–230, 2015.

[9] Z. Wang, N. Zhang, J. Ding, C. Lu, and Y. Jin, "Experimental study on wind erosion resistance and strength of sands treated with microbial-induced calcium carbonate precipitation," *Advances in Materials Science and Engineering*, vol. 2018, Article ID 3463298, 10 pages, 2018.

[10] L. A. Van Paassen, M. P. Harkes, G. A. Van Zwieten, W. H. Van der Zon, W. R. L. Van der Star, and M. C. M. Van Loosdrecht, "Scale up of BioGrout: a biological ground reinforcement method," in *Proceedings of the 17th International Conference on Soil Mechanics and Geotechnical Engineering*, pp. 2328–2333, Lansdale IOS Press, Alexandria, Egypt, October 2009.

[11] N. Zhang and Z. Wang, "Review of soil thermal conductivity and predictive models," *International Journal of Thermal Sciences*, vol. 117, pp. 172–183, 2017.

[12] J. C. Choi, S. R. Lee, and D. S. Lee, "Numerical simulation of vertical ground heat exchangers: intermittent operation in unsaturated soil conditions," *Computers and Geotechnics*, vol. 38, no. 8, pp. 949–958, 2011.

[13] X. B. Yu, A. Pradhan, N. Zhang, B. Thapa, and S. Tjuatja, "Thermo-TDR probe for measurement of soil moisture, density, and thermal properties," in *Proceedings of 2014 GeoCongress*, pp. 2804–2813, Atlanta, GA, USA, 2014.

[14] X. B. Yu, N. Zhang, and A. Pradhan, "Development and evaluation of a thermo-TDR probe," in *Proceedings of 2014 Geoshanghai International Conference*, pp. 434–444, Shanghai, China, 2014.

[15] X. B. Yu, N. Zhang, A. Pradhan, B. Thapa, and S. Tjuatja, "Design and evaluation of a thermo-TDR probe for geothermal applications," *Geotechnical Testing Journal*, vol. 38, no. 6, pp. 864–877, 2015.

[16] R. M. Gangadhara and D. N. Singh, "A generalized relationship to estimate thermal resistivity of soils," *Canadian Geotechnical Journal*, vol. 36, no. 4, pp. 767–773, 1999.

[17] J. Pan and Y. G. Wang, "Numerical simulation of measurement of thermal conductivity with transient hot wire method," *Journal of China Jiliang University*, vol. 19, no. 2, pp. 108–113, 2008, in Chinese.

[18] O. Johansen, *Thermal conductivity of soils*, Ph.D. thesis, US Army Corps of Engineers, Cold Regions Research and Engineering Laboratory, University of Trondheim, Trondheim, Norway, 1975.

[19] J. Côté and J.-M. Konrad, "A generalized thermal conductivity model for soils and construction materials," *Canadian Geotechnical Journal*, vol. 42, no. 2, pp. 443–458, 2005.

[20] N. Zhang, X. B. Yu, A. Pradhan, and A. J. Puppala, "Thermal conductivity of quartz sands by thermo-TDR probe and model prediction," *ASCE Journal of Materials in Civil Engineering*, vol. 27, no. 12, article 0401509, 2015.

[21] S. X. Chen, "Thermal conductivity of sands," *Heat and Mass Transfer*, vol. 44, no. 10, pp. 1241–1246, 2008.

[22] M. S. Kersten, *Laboratory Research for the Determination of the Thermal Properties of Soils, Bulletin No. 28*, University of Minnesota Engineering Experiment Station, Minneapolis, MN, USA, 1949.

[23] W. O. Smith, "The thermal conductivity of dry soil," *Soil Science*, vol. 53, no. 6, pp. 435–460, 1942.